October 2025
Volume 1
Issue 4

DOI: 10.48308/ijce.2025.107012

Interdisciplinary Journal of Civil Engineering
Shahid Beheshti University

Assessment of Seismic Collapse Capacity in Special Moment-Resisting Frames Designed via Equivalent Lateral Force and Response Spectrum Procedures Under ASCE 7-22 and FEMA P-695 Frameworks

Authors:

Parsa Rashvand[1], Mohammadjavad Hamidia[1,*], Nemat Hassani[1]

Abstract

Steel special moment-resisting frame (SMRFs) are considered one of the most widely used seismic force-resisting systems in earthquake-prone regions, designed to provide high ductility and energy dissipation capacity. In this study, the effect of the initial structural design method on the collapse capacity of this system was investigated. For this purpose, three structures with 2, 4, and 8 stories were designed in accordance with the provisions of ASCE 7-22 using both the equivalent lateral force (ELF) method and the response spectrum analysis (RSA) method in ETABS software, and the required member sections were obtained. Subsequently, the developed models were transferred to the OpenSees platform and subjected to modal analysis, nonlinear static analysis, and incremental dynamic analysis (IDA). For the Incremental Dynamic Analysis, 44 far-field earthquake ground motion records recommended in FEMA P695 were employed. In total, more than 9,000 nonlinear time-history analyses were conducted to develop fragility curves and calculate the collapse margin ratio (CMR). The obtained results indicate that the initial analysis and design method has a significant effect on the final nonlinear structural response and the probability of collapse at high seismic intensity levels. In all models, structures designed using the equivalent lateral force method exhibited higher collapse margin ratios compared to those designed using the response spectrum analysis method, indicating greater seismic capacity and higher safety margins against collapse.

Keywords: Steel Moment-Resisting Frame, Collapse Margin Ratio, ASCE 7-22 Standard, Incremental Dynamic Analysis, Fragility Curves, FEMA P695 Methodology

1. Faculty of Civil, Water, and Environmental Engineering, Shahid Beheshti University, Tehran, Iran

*Corresponding Author: m_hamidia@sbu.ac.ir

1. Introduction

Steel moment-resisting frames (MRFs) have been used since the mid-twentieth century as one of the most common seismic force-resisting systems in structures. Initially, the design focus of these systems was mainly on providing sufficient stiffness and initial strength against lateral loads. However, the occurrence of severe earthquakes, including the 1971 San Fernando earthquake (Jennings, 1971), the 1994 Northridge earthquake (Hall et al., 1995; Hauksson et al., 1995; Hough et al., 2024), and the 1995 Kobe earthquake (Hassani & Takada, 1995; Hassani et al., 1995; Koketsu, 1996; Popov et al., 1998), revealed fundamental weaknesses in the connections of steel moment frames. Brittle and progressive failures in beam-column connections led to extensive revisions in design provisions and ultimately resulted in the development of special steel moment-resisting frames (SMRFs). These frames, due to their high ductility, significant energy dissipation capacity, and desirable post-yield behavior, play a key role in the seismic design of structures located in regions with high seismicity. Standards such as AISC 341-22 (AISC, 2022) and ASCE 7-22 (ASCE, 2022) provide specific requirements regarding component design, connection detailing, and seismic force distribution in order to ensure the proper performance of these structures at different performance levels. In ASCE 7-22, two methods, namely the equivalent lateral force (ELF) method and the response spectrum analysis (RSA) method, are presented for the seismic design of structures. The ELF method is still widely used in conventional projects due to its simplicity and extensive practical background. In contrast, the RSA method, by providing a more accurate representation of the modal distribution of structural response, offers greater analytical accuracy. Nevertheless, in practice, the difference in the performance of structures designed using these two methods, particularly in terms of nonlinear behavior and collapse probability, has rarely been investigated comprehensively. With the advancement of performance-based seismic design approaches, the realistic assessment of structural collapse probability under severe earthquakes has gained increasing importance. The use of incremental dynamic analysis (IDA), the development of fragility curves, and the calculation of indices such as the collapse margin ratio (CMR) provide powerful tools for the detailed evaluation of seismic collapse performance in structures (Vamvatsikos & Cornell, 2002; Shafaei & Naderpour, 2022; Farsangi et al., 2016; Hojatirad & Naderpour, 2021; Naderpour et al., 2020; Hamidia et al., 2014a, 2014b, 2015, 2022). In this study, three special steel moment-resisting frames with 2, 4, and 8 stories were selected as representative examples of low-rise, mid-rise, and high-rise buildings, as well as structures with short and long fundamental periods. For each structure, the design was carried out in accordance with ASCE 7-22 using both the ELF and RSA methods in ETABS (CSI, 2024), and the optimal member sections were obtained. Subsequently, the six resulting models were developed in OpenSees (McKenna, 2011; Mazzoni et al., 2006), where nonlinear static and dynamic analyses were performed. Parameters such as the first-mode period and base shear were extracted, and pushover curves were generated. Thereafter, using the earthquake ground motion record set proposed in FEMA P-695 (FEMA, 2009), IDA analyses were conducted, and the 16th, 50th, and 84th percentile fractiles were plotted. Fragility curves were

also developed. Finally, the CMR index was calculated and compared as the primary criterion for evaluating the collapse probability of the structures. The main objective of this study is to perform a comparative assessment of the seismic performance of special steel moment-resisting frames designed using the ELF and RSA methods at different height levels and to evaluate their collapse probability through nonlinear analyses. The findings of this study can contribute significantly to a better understanding of the actual structural behavior, the selection of appropriate design methods, and the improvement of seismic safety in the design of special steel moment-resisting frames.

2. Configuration of Structural Buildings and Design Procedures

In this study, in order to evaluate the seismic collapse capacity of special steel moment-resisting frames and considering the recent modifications in the ASCE 7-22 and AISC (358-22, 341-22, and 360-22) standards (AISC, 2022a, 2022b; AISC Committee, 2022), the use of previously validated structural models was not sufficient to satisfy the objectives of the research. Therefore, new structural models with different heights, including 2-, 4-, and 8-story buildings, were designed in ETABS in accordance with the updated provisions and analyzed using the equivalent lateral force and response spectrum analysis methods in order to obtain the required sections for nonlinear modeling and analysis in OpenSees. The structures were regular in plan and consisted of three equal spans in both the X and Y directions, with each span measuring 5 m. The height of the first story was considered 3.5 m in all models, while the upper stories had a height of 3.2 m. The lateral force-resisting system in both directions consisted of special steel moment-resisting frames, and the structures were categorized as highly ductile systems with extensive nonlinear behavior. As presented in Appendix A Table A1, W-shaped sections made of ASTM A992 Grade 50 steel were used for the main structural members, including beams and columns, in accordance with the sixteenth edition of the AISC steel construction standard (AISC, 2022). The mechanical properties of this steel include a yield stress (F_y) of 345 MPa, an ultimate tensile stress (F_u) of 450 MPa, a modulus of elasticity (E) of 200,000 MPa, and a Poisson's ratio (v) of 0.3. According to FEMA P-695 (FEMA, 2009), in the design of special steel moment-resisting frames, the dead load and exterior wall load were considered as 440 and 122 kg/m², respectively, for all stories. The live load was taken as 100 kg/m² for the roof and 245 kg/m² for the remaining stories. The buildings were assumed to have office occupancy and to be located on site class D with a seismic hazard level of D_{max}. The calculated fundamental periods (T), based on the relation:

$$T = C_u T_a = C_u C_t h_n^x \tag{1}$$

The fundamental period values are presented in Table 1 and were used for the design process.

Table 1. Maximum and minimum seismic design category (SDC) criteria.

No. Stories	Design Analysis Procedure	SDC	Fundamental Period (sec)
2	ELF	D_{max}	0.46
4	ELF	D_{max}	0.79
8	ELF	D_{max}	1.36
2	RSA	D_{max}	0.52
4	RSA	D_{min}	0.86
8	RSA	D_{min}	1.48

To determine the seismic response spectrum, the seismic hazard parameters corresponding to the D_{max} hazard level were adopted from FEMA P695. In addition, according to ASCE 7-22, the transition period is obtained from the ratio of the spectral response acceleration parameter at a 1-second period to that at the short period, as follows:

$$T_s = \frac{S_{D1}}{S_{DS}} = \frac{S_{M1}}{S_{MS}} \tag{2}$$

For the D_{max} seismic hazard level, the value of this transition period was equal to 0.6 s. Structures with a fundamental period shorter than T_s were classified as short-period structures, whereas those with a fundamental period longer than T_s were categorized as long-period structures. Therefore, based on Table 1, the modeled 2-story structures were classified as short-period structures, while the modeled 4- and 8-story structures were classified as long-period structures. Furthermore, the principal design spectrum parameters were considered as S_s = 1.5 g and F_a = 1 for short-period structures, and S_1 = 0.6 g and F_v = 1.5 for long-period structures. The seismic weight was also calculated from the sum of 1.05 times the dead load and 0.25 times the live load. Table 2 presents the seismic design parameters of the structural models, including design base shear, seismic coefficient, structural height, and first-mode period according to the design analysis method used (equivalent lateral force or response spectrum analysis).

Table 2. Seismic design characteristics of the designed structures.

No. stories	Design analysis procedure	SDC	Height (m)	First mode period (sec)	Seismic coefficient (g)	Seismic weight (kN)	Design base shear (kN)
2	ELF	D_{max}	6.7	0.65	0.1875	963.7	180.69
4	ELF	D_{max}	13.1	0.82	0.1427	2303.44	328.66
8	ELF	D_{max}	25.9	1.52	0.0827	3845.11	318.03

2	RSA	D_{max}	6.7	0.80	0.1875	941.9	176.61
4	RSA	D_{min}	13.1	1.25	0.1308	1889.31	269.57
8	RSA	D_{min}	25.9	1.64	0.076	3835.26	317.21

3. Nonlinear Structural Modeling

The nonlinear modeling and analysis of the structures in this study were carried out in OpenSees by selecting the frame in the X direction and considering the seismic behavior of the structure under lateral loading. The interior frames were designed solely to resist gravity loads and were therefore not included in the lateral modeling. The column base supports were assumed to be fully fixed, and all analyses were conducted in a two-dimensional space. The P-Delta effect (Adam et al., 2004) was considered in the analyses in order to account for the secondary stability effects of the structures. This effect was simulated using columns without lateral stiffness that were modeled as rigid members with no lateral resistance. Although these columns did not directly contribute to the lateral behavior of the structure, they transferred the nonlinear effects associated with the maximum inter-story drift ratio. The seismic mass of the structure was defined as concentrated masses at the beam-to-column joint nodes, thereby accounting for the dynamic mass distribution of the structure within the model. To consider damping effects, the Rayleigh damping model, which includes both mass and stiffness matrices, was adopted. In accordance with the recommendations of FEMA P-695 (FEMA, 2009), a damping ratio of 5% was considered, which is appropriate for evaluating the seismic collapse performance of structural systems. According to ASCE 7-22 (ASCE, 2022), in designs based on response spectrum analysis, a sufficient number of vibration modes must be considered such that at least 90% of the effective modal mass participation is achieved in each principal direction of earthquake excitation in order to properly capture the dynamic response of the structure. Structural members, including beams and columns, were modeled using the NonlinearBeamColumn element to accurately represent nonlinear flexural behavior. The behavior of steel materials was defined using the Steel02 material model, which supports hysteretic behavior with both kinematic and isotropic hardening and is capable of simulating cyclic loading and unloading behavior. The beam-column panel zone was also designed to satisfy the required strength provisions in accordance with ANSI/AISC 341-22 (AISC, 2022).

4. Nonlinear Analyses

4.1. Nonlinear Static Analysis (Pushover)

In order to evaluate the nonlinear capacity of the special steel moment-resisting frames modeled in this study, pushover analysis was performed incrementally and in a controlled manner based on the horizontal roof displacement of the structure in OpenSees. The objective

of this analysis is to investigate the overall structural behavior under increasing lateral loads up to the point of collapse and instability. In this analysis, the lateral load was calculated according to Eq. (3) and distributed in a triangular pattern along the height of the structure and applied at the floor nodes.

$$F_x = m_x \phi_{1,x} \tag{3}$$

where F_x, m_x , and $\phi_{1,x}$ represent the lateral force, mass, and mode shape, respectively. During the analysis process, the structure initially behaves linearly, then enters the yielding phase, and with continued loading experiences stiffness degradation and eventually strength deterioration. The base shear-to-weight ratio versus roof displacement-to-height ratio (in percent) was extracted separately for each model, and the nonlinear behavior of the structures was compared. The overall shape of the curves for all six models shows a continuous transition from elastic behavior to instability (collapse), although the level of maximum displacement and lateral resistance differs significantly between models. These curves can also be used to calculate strength-related indices (overstrength factor), ductility, and even relative collapse capacity. Furthermore, these results can serve as a basis for estimating structural response under nonlinear dynamic analyses such as incremental dynamic analysis or for deriving fragility curves. Figure 1 presents the idealized story-wise pushover curves for 2-, 4-, and 8-story structures designed using both equivalent static analysis and response spectrum analysis procedures.

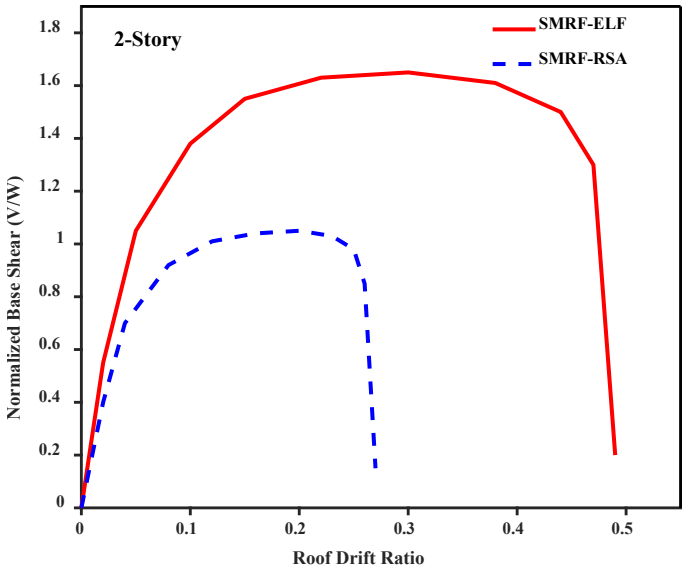

(a)

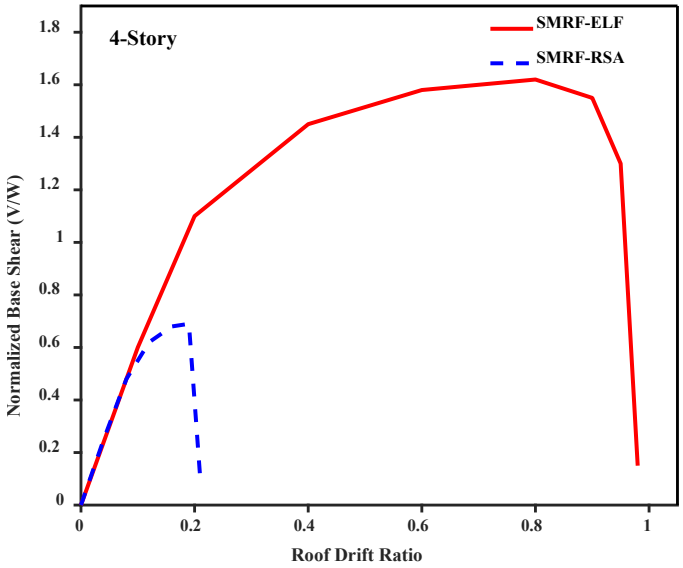

(b)

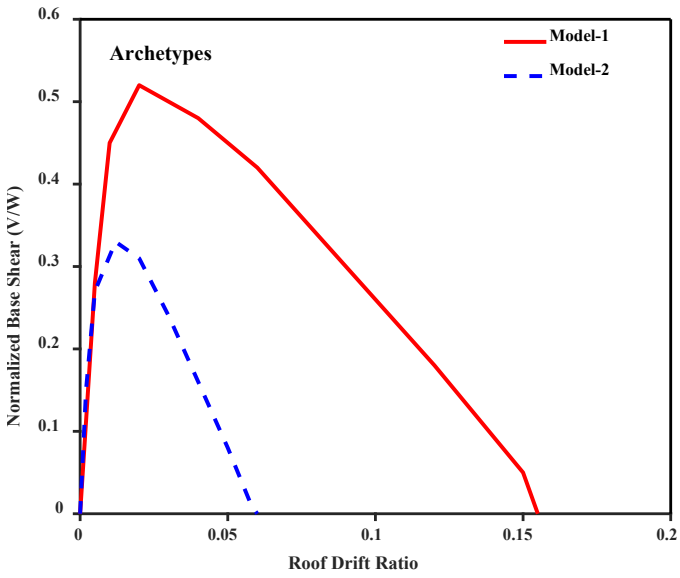

(c)

Figure 1. Pushover curves for the designed structures; (a) 2-story structures, (b) 4-story structures, (c) 8-story structures.

4.2. Incremental Dynamic Analysis (IDA)

4.2.1. Extraction of IDA Curves

In this section, in order to investigate the structural behavior in the collapse range, incremental nonlinear dynamic analysis was performed for the 2-, 4-, and 8-story models. This analysis method involves applying a set of earthquake ground motion records to the nonlinear structural model, with progressively increasing intensity until structural instability and collapse are reached. In this study, as shown in Table 3, a set of 44 far-field earthquake ground motion records recommended by FEMA P695 was used. The selected records include earthquakes generated by strike-slip and reverse (thrust) fault mechanisms, recorded on site classes C (soft rock) and D (stiff soil). The rupture distances of the recording stations range from 11.4 km to 26.4 km, with an average distance of 16.4 km. The peak ground acceleration (PGA) ranges from 0.21g to 0.82g, and the moment magnitudes of the earthquakes vary between 6.5 and 7.6.

Table 3. Characteristics of FEMA P695 far-field ground motions (FEMA, 2009).

No. of record	Name	M_w	PGA_{max} (g)	PGV_{max} (cm/s)	Station	Orientation
1-2	Northridge	6.7	0.52	63	Beverly Hills–14,145 Mulholland	009-279
3-4	Northridge	6.7	0.48	45	Canyon County–W Lost Canyon	000-270
5-6	Duzce, Turkey	7.1	0.82	62	Bolu	000-090
7-8	Hector Mine	7.1	0.34	42	Hector	000-090
9-10	mperial Valley	6.5	0.35	33	Delta	262-352
11-12	mperial Valley	6.5	0.38	42	El Centro Array #11	140-230
13-14	Kobe, Japan	6.9	0.51	37	Nishi—Akashi	000-090
15-16	Kobe, Japan	6.9	0.24	38	Shin-Osaka	000-090
17-18	Kocaeli, Turkey	7.5	0.36	59	Duzce	180-270
19-20	Kocaeli, Turkey	7.5	0.22	40	Arcelik	000-090
21-22	Landers	7.3	0.24	52	Yermo Fire Station	270-360
23-24	Landers	7.3	0.42	42	Coolwater	Long-Trans
25-26	Loma Prieta	6.9	0.53	35	Capitola	000-090
27-28	Loma Prieta	6.9	0.56	45	Gilroy Array #3	000-090
29-30	Manjil, Iran	7.4	0.51	54	Abbar	Long-Trans
31-32	Superstition Hills	6.5	0.36	46	El Centro Imp.Co. Center	000-090
33-34	Superstition Hills	6.5	0.45	36	Poe Road	270-360
35-36	Cape Mendocino	7	0.55	44	Rio Dell Overpass	270-360

37-38	Chi-Chi, Taiwan	7.6	0.44	115	CHY101	W-N
39-40	Chi-Chi, Taiwan	7.6	0.51	39	TCU045	W-N
41-42	San Fernando	6.6	0.21	19	LA Hollywood Stor Lot	090-180
43-44	Friuli, Italy	6.5	0.35	31	Tolmezzo	000-270

The intensity of ground motions in the IDA analysis was incrementally increased using a fixed-step algorithm until the structure reached collapse. The use of fixed incremental steps, while maintaining accuracy in identifying the critical intensity level, reduces the number of required analyses. At each step, a complete nonlinear time-history analysis was performed, and response parameters such as inter-story drift ratios were calculated. In this study, the maximum interstory drift ratio was adopted as the damage index, and the collapse threshold was defined as 10%, based on previous research in this field. Figures 2 and 3 respectively present the IDA curves for the 2-, 4-, and 8-story structures designed using the equivalent lateral force method and the response spectrum analysis method. For ductile structural systems such as those studied here, the relationship between seismic intensity and damage index initially shows an increasing trend, and as the structure enters the softening region, the curve tends to flatten. This behavior is interpreted as an indicator of collapse or dynamic instability.

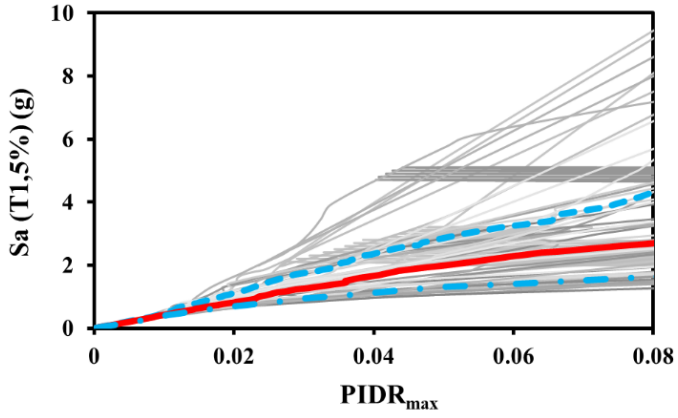

(a)

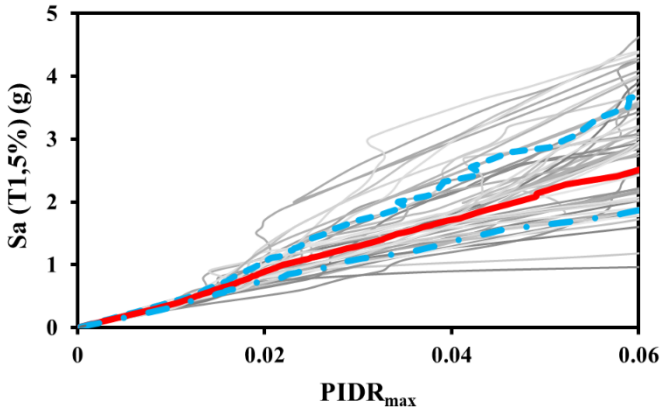

(b)

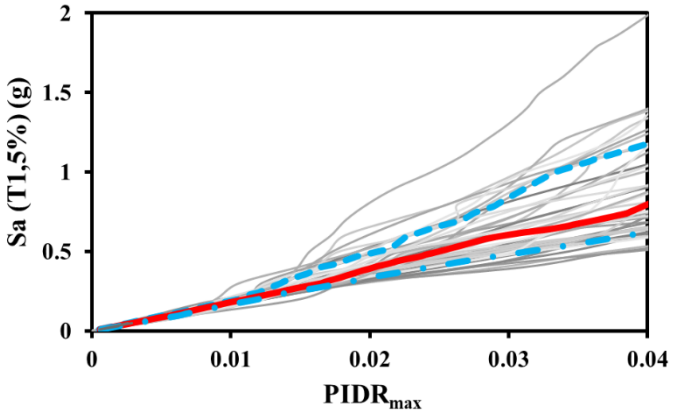

(c)

Figure 2. IDA curves for structures designed based on the equivalent lateral force method; (a) 2-story structure, (b) 4-story structure, (c) 8-story structure.

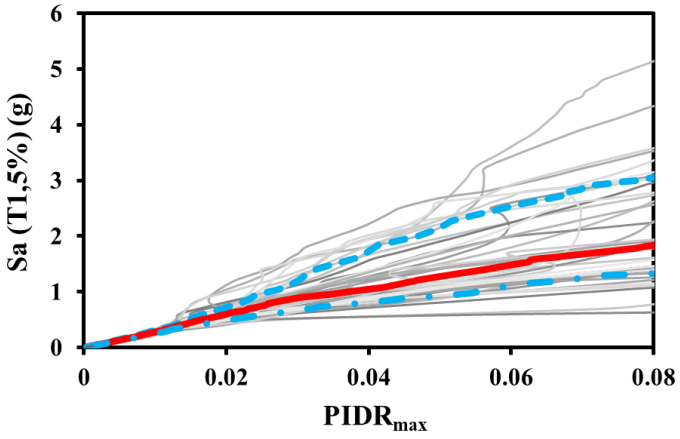

(a)

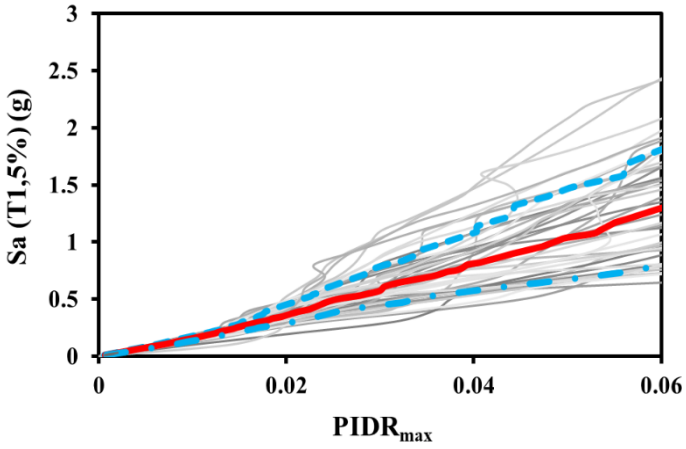

(b)

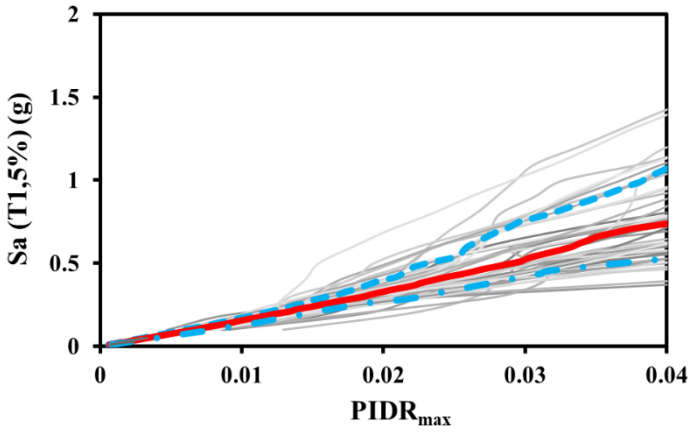

(c)

Figure 3. IDA curves for structures designed based on the response spectrum analysis method; (a) 2-story structure, (b) 4-story structure, (c) 8-story structure.

The resulting curves were also plotted for the 16th, 50th (median), and 84th fractiles to evaluate the variability and dispersion of structural response at different probability levels.

4.2.2. Extraction of Fragility Curves and Calculation of CMR Values

In order to statistically evaluate the seismic collapse probability of the investigated structures, fragility curves were derived based on the results of incremental nonlinear dynamic analyses. A fragility curve is a probabilistic function of earthquake intensity and the probability of exceeding a specific limit state, such as dynamic collapse or lateral instability. To model these curves statistically, the data obtained from IDA analyses for 44 far-field ground motion records and the corresponding collapse intensity values were extracted. According to FEMA P58 (FEMA, 2018), the seismic collapse data points are fitted to a log-normal distribution with median (μ) and logarithmic standard deviation (σ) parameters in order to determine these values. The statistical model used for the fragility curves is a lognormal distribution, and the probability of collapse at a given intensity measure (IM) is calculated using Eq (4):

$$P(\text{Collapse}|IM = im) = \Phi\left[\frac{1}{\beta}\left(\ln(im) - \mu\right)\right] \tag{4}$$

where in Eq. (4), the standard normal cumulative distribution is denoted by Φ, while β represents the standard deviation of natural logarithm of the im, ln(im). Here, μ corresponds to the median of ln(IM). CMR [64-74] is the ratio of median collapse capacity to MCE demand, as expressed in Eq. (5).

$$\text{CMR} = \frac{\hat{S}_{CT}}{S_{MT}} \tag{5}$$

Table 4 presents the calculated values of S_{MT}, $\hat{S}_{CT}$, and CMR for structures designed using either the equivalent lateral force method or the response spectrum analysis method, and also compares the percentage differences in collapse performance.

Table 4. Seismic collapse evaluation and quantification results of the structures.

No. stories	Design analysis procedure	S_{MT}	$\hat{S}_{CT}$	CMR
2	ELF	1.5	4.15	2.77
2	ELF	1.5	3	2
4	ELF	1.4	6.45	4.61
4	RSA	1.4	3.3	2.36
8	RSA	0.66	3.8	5.75
8	RSA	0.66	2.7	4.09

Figures 4 and 5 respectively present the fragility curves and CMR values for the 2-, 4-, and 8-story structures designed using the equivalent lateral force method and the response spectrum analysis method.

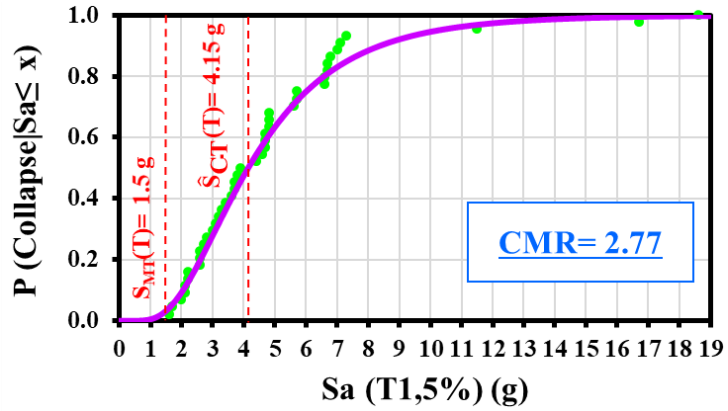

(a)

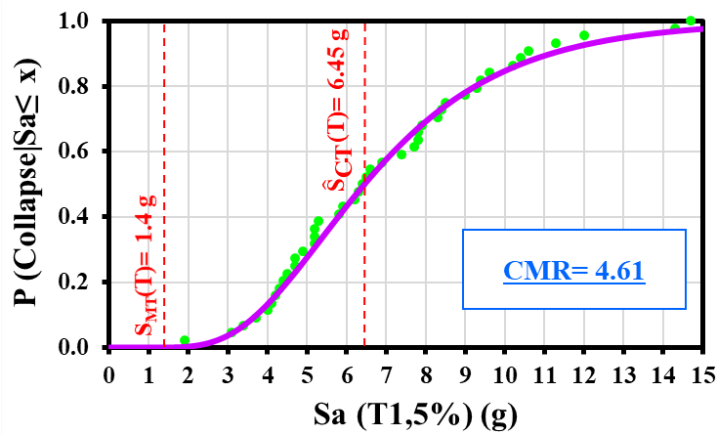

(b)

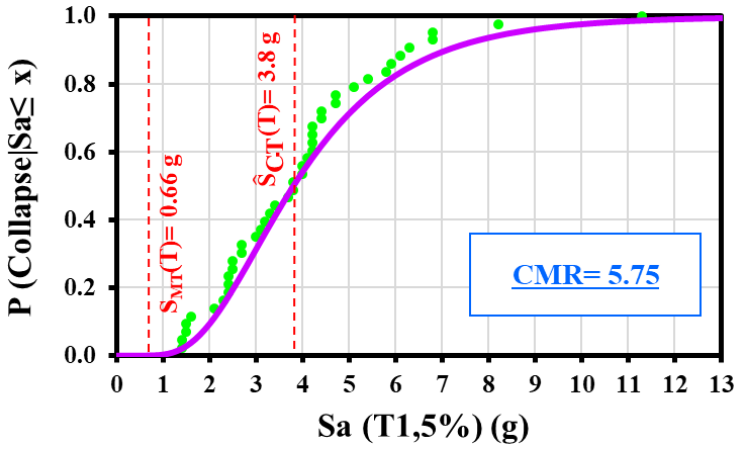

(c)

Figure 4. Fragility curves for structures designed based on the ELF method; (a) 2-story structure, (b) 4-story structure, (c) 8-story structure.

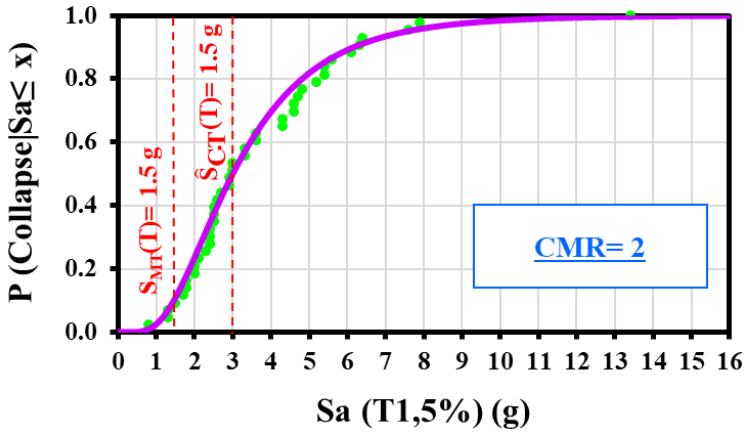

(a)

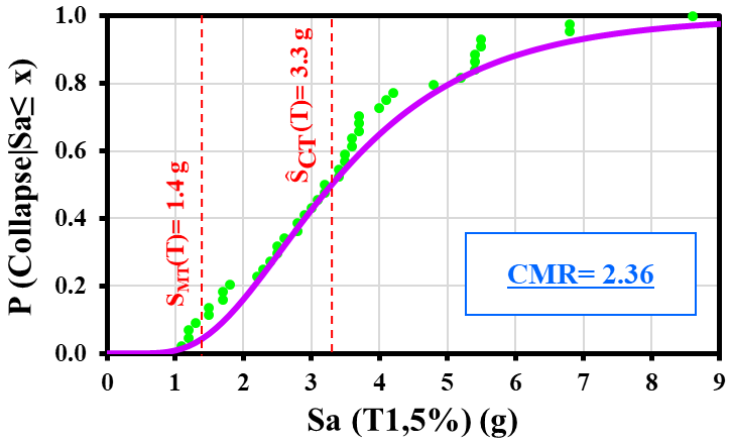

(b)

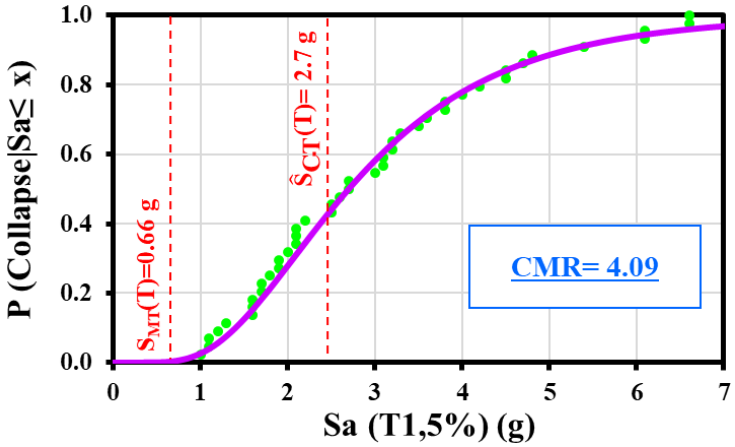

(c)

Figure 5. Fragility curves for structures designed based on the RSA method; (a) 2-story structure, (b) 4-story structure, (c) 8-story structure.

5. Summary and Conclusions

In this study, special steel moment-resisting frames were designed based on the equivalent lateral force (ELF) and response spectrum analysis (RSA) methods in accordance with the ASCE 7-22 standard, and their seismic behavior was then investigated and compared. Structures with 2, 4, and 8 stories were designed, modeled, and analyzed. After performing nonlinear static and incremental dynamic analyses, fragility curves and the collapse margin ratio (CMR) were obtained as collapse performance indicators. The key findings are summarized as follows:

I. Based on the pushover curve results, structures designed using the ELF method, due to heavier sections and higher stiffness compared to those designed using the RSA method, exhibited greater ultimate displacement capacity. On the other hand, structures designed using the RSA method showed more gradual and ductile nonlinear behavior in the initial response phase, which may lead to better energy dissipation and a more uniform distribution of damage prior to collapse. In taller models (8-story), a gradual and continuous stiffness degradation after yielding was observed, indicating stable and ductile behavior under severe seismic loading. In contrast, shorter models (2-story) experienced a sudden strength degradation after yielding, indicating more brittle behavior.

II. In all studied models, structures designed based on the RSA method showed improved seismic capacity against severe earthquakes prior to reaching the 10% interstory drift collapse threshold. IDA results indicated that ELF-designed models exhibited more scattered responses to different ground motions and were more sensitive to the dynamic characteristics of the records. For example, in the 4-story model, the RSA-designed structure experienced lower nonlinear drift under the same intensity levels, and its IDA curves showed more stable behavior compared to the corresponding ELF model. These

results clearly indicate better control of nonlinear displacements and higher resistance in RSA-based design compared to ELF.

III. Based on the fragility curves obtained from IDA analyses, the collapse probability of RSA-designed structures was significantly lower than that of ELF-designed structures across all heights. Approximately, the collapse probability for ELF-designed structures was estimated to be about 2 to 3 times higher than that of RSA. These results indicate that RSA-based design not only increases seismic capacity under strong earthquakes but also reduces response dispersion, thereby improving reliability in predicting behavior near the collapse limit state.

IV. The CMR values increased with the number of stories. This increase is attributed to the use of stiffer and stronger sections in taller structures to control lateral displacement, which resulted in higher collapse resistance. Additionally, comparison between the two methods showed that CMR values for the ELF method (ranging from 2.77 to 5.75) were higher than those for the RSA method (ranging from 2 to 4.09). This difference can be attributed to the more conservative nature of the ELF method, which applies seismic forces based on simplified assumptions and amplification factors. In contrast, the RSA method, by considering a more realistic modal force distribution and higher-mode participation, results in lower predicted collapse capacity and therefore provides a more conservative seismic assessment compared to ELF.

Overall, the results of this study indicate that the choice of seismic analysis method can significantly affect the estimated collapse capacity and safety margin of structures against global failure. These differences should also be considered in the development of collapse-resistant design provisions.

Data Statement

Data will be made available on reasonable request.

Conflict of Interest

The authors declare that there is no conflict of interest regarding the publication of this paper.

Appendix A

Table A1 Designed member cross-sections for structural buildings.

Building ID	Story number	Analysis method	Beam section	Column section
2	1	ELF	W24x76	W14x193
	2	ELF	W21x62	W14x193
4	1	ELF	W21x111	W14x233

	2	ELF	W21x111	W14x233
	3	ELF	W18x76	W14x145
	4	ELF	W18x76	W14x145
8	1	ELF	W18x76	W18x234
	2	ELF	W18x76	W18x234
	3	ELF	W18x76	W12x152
	4	ELF	W18x76	W12x152
	5	ELF	W18x60	W12x152
	6	ELF	W18x60	W12x152
	7	ELF	W18x60	W12x152
	8	ELF	W18x60	W12x152
2	1	RSA	W21x62	W14x145
	2	RSA	W18x55	W14x145
4	1	RSA	W18x76	W14x176
	2	RSA	W18x76	W14x176
	3	RSA	W16x57	W14x120
	4	RSA	W16x57	W14x120
8	1	RSA	W21x73	W14x233
	2	RSA	W21x73	W14x233
	3	RSA	W21x73	W14x233
	4	RSA	W21x73	W14x233
	5	RSA	W16x57	W14x145
	6	RSA	W16x57	W14x145
	7	RSA	W16x57	W14x145
	8	RSA	W16x57	W14x145

6. References

Adam, C., Ibarra, L. F., & Krawinkler, H. (2004). *Evaluation of P-delta effects in non-deteriorating MDOF structures from equivalent SDOF systems*. Stanford University.

AISC. (2022a). *Prequalified connections for special and intermediate steel moment frames for seismic applications* (ANSI/AISC 358-22). American Institute of Steel Construction.

AISC. (2022b). *Seismic provisions for structural steel buildings* (ANSI/AISC 341-22). American Institute of Steel Construction.

AISC Committee. (2022). *Specification for structural steel buildings* (ANSI/AISC 360-22). American Institute of Steel Construction.

American Society of Civil Engineers. (2022). *Minimum design loads and associated criteria for buildings and other structures*. Author.

Computers and Structures, Inc. (2024). *ETABS user's manual* (Version 20.0.0). Author.

Farsangi, E. N., Yang, T. Y., & Tasnimi, A. A. (2016). Influence of concurrent horizontal and vertical ground excitations on the collapse margins of non-ductile RC frame buildings. *Structural Engineering and Mechanics: An International Journal, 59*(4), 653–669.

FEMA. (2009). *Quantification of building seismic performance factors* (FEMA P-695). Federal Emergency Management Agency.

FEMA. (2018). *Seismic performance assessment of buildings, Volume 1 – Methodology* (FEMA P-58-1). Federal Emergency Management Agency.

Hall, J. F., Holmes, W. T., & Somers, P. (1995). *Northridge earthquake of January 17, 1994: Reconnaissance report* (Vol. 1). Earthquake Engineering Research Institute.

Hamidia, M., Filiatrault, A., & Aref, A. (2014a). Simplified seismic sidesway collapse analysis of frame buildings. *Earthquake Engineering & Structural Dynamics, 43*(3), 429–448.

Hamidia, M., Filiatrault, A., & Aref, A. (2014b). Simplified seismic sidesway collapse capacity-based evaluation and design of frame buildings with linear viscous dampers. *Journal of Earthquake Engineering, 18*(4), 528–552.

Hamidia, M., Filiatrault, A., & Aref, A. (2015). Seismic collapse capacity–based evaluation and design of frame buildings with viscous dampers using pushover analysis. *Journal of Structural Engineering, 141*(6), 04014153.

Hamidia, M., Shokrollahi, N., & Ardakani, R. R. (2022). The collapse margin ratio of steel frames considering the vertical component of earthquake ground motions. *Journal of Constructional Steel Research, 188*, 107054.

Hassani, N., & Takada, S. (1995). Lifelines performance and damage during 17 Jan. 1995, South Hyogo Great Earthquake. In *Proceedings of the first Iran–Japan Workshop on Recent Earthquakes in Iran and Japan* (pp. 1809–1821).

Hassani, N., Takada, S., & Mostafa, A. A. (1995). Quick report of main damage caused by the 1995 Hyogo-ken Nambu earthquake. *Journal of Natural Disaster Science, 16*(3), 59–70.

Hauksson, E., Jones, L. M., & Hutton, K. (1995). The 1994 Northridge earthquake sequence in California: Seismological and tectonic aspects. *Journal of Geophysical Research: Solid Earth, 100*(B7), 12335–12355.

Hojatirad, A., & Naderpour, H. (2021). Seismic assessment of RC structures having shape memory alloys rebar and strengthened using CFRP sheets in terms of fragility curves. *Bulletin of Earthquake Engineering, 19*(12), 5087–5112.

Hough, S. E., Graves, R. W., Cochran, E. S., Yoon, C. E., Blair, L., Haefner, S., … Quitoriano, V. (2024). The 17 January 1994 Northridge, California, earthquake: A retrospective analysis. *The Seismic Record, 4*(3), 151–160.

Jennings, P. C. (1971). *Engineering features of the San Fernando earthquake of February 9, 1971* (Vol. 71, No. 2). California Institute of Technology, Earthquake Engineering Research Laboratory.

Koketsu, K. (1996). Damaging earthquakes in California and 1995 Kobe earthquake. *Science Journal, 66*, 93–97.

Mazzoni, S., McKenna, F., Scott, M. H., & Fenves, G. L. (2006). OpenSees command language manual. *Pacific Earthquake Engineering Research (PEER) Center, 264*(1), 137–158.

McKenna, F. (2011). OpenSees: A framework for earthquake engineering simulation. *Computing in Science & Engineering, 13*(4), 58–66.

Naderpour, H., Kiani, A., & Kheyroddin, A. (2020). Structural control of RC buildings subjected to near-fault ground motions in terms of tuned mass dampers. *Scientia Iranica, 27*(1), 122–133.

Popov, E. P., Yang, T. S., & Chang, S. P. (1998). Design of steel MRF connections before and after 1994 Northridge earthquake. *Engineering Structures, 20*(12), 1030–1038.

Shafaei, H., & Naderpour, H. (2022). Collapse capacity of ordinary RC moment frames considering mainshock-aftershock effects. *Journal of Earthquake Engineering, 26*(10), 5318–5337.

Vamvatsikos, D., & Cornell, C. A. (2002). Incremental dynamic analysis. *Earthquake Engineering & Structural Dynamics, 31*(3), 491–514.